Carpathian Journal of Earth and Environmental Sciences, February 2016, Vol. 11, No. 1, p. 153 - 166

ESTIMATION OF SOIL EROSION IN NORTHERN KIRKUK GOVERNORATE, IRAQ USING RUSLE, REMOTE SENSING AND GIS

Alaa M. Atiaa AL-ABADI, Hussein B. GHALIB & Wasan S. AL-QURNAWI

Department of Geology, College of Sciences, University of Basra, Basra, Iraq.Corresponding author: Hussein B. Ghalib <hbggeo@gmail.com>

Abstract: A quantitative assessment of annual soil erosion by water in the northern part of Kirkuk Governorate, north of Iraq was investigated through integration of remote sensing, GIS and empirical RULSE soil erosion model. The five factors of RULSE model (rainfall erosivity R, soil erodibility K, slope length and steepness LS, crop management C, and practice factor P) were derived from different resources such as field survey, archival data, digital elevation model, and LANDSAT 8 multi-bands imagery. The annual soil erosion loss was estimated by multiplying the five factors in raster format using raster calculator of ArcGIS 10.2 software. The estimated annual soil losses rate for the study area ranges from 0 to 245 (t ha^{-1} yr^{-1}) with an average of 2 (t ha^{-1} yr^{-1}). The value ranges were classified into four categories: minimal, low, moderate, high soil erosion hazard zones using four classification schema: quantile, natural breaks, geometric, and standard deviation. Due to the similarity of results, the comparison was carried out between two schemas: natural breaks and geometric. The area covered by minimal-low soil hazard zones extends over an area of about 88% and 99% based on geometric and natural breaks schema, respectively. In turn, the moderate-high soil hazard zones cover only very small area (0.3%) based on natural breaks and relatively small area (12%) depending on geometric scheme. In general, both method results indicate that hazard of soil erosion is low in the study area. The spatial pattern of classified soil erosion rate indicates that the areas at moderate to high risk is located in the northeast and very small area in the east, while the minimal to low zones cover the other parts. The obtained results of could be useful to implement soil conservation practices in the study area.

Key words: RUSLE, GIS, NDVI, Kirkuk, Iraq, soil erosion.

1. INTRODUCTION

Soil erosion by water is a world major problem that results in decrease of soil fertility, land degradation, and also affecting the sustainability and productivity of agricultural areas. In fact, soil erosion is a geomorphological process driven by natural forces, and it could be accelerated by human activities such as deforestation, construction, agriculture, and mining. To quantify soil rate, techniques such as erosion modeling can be helpful. Soil erosion modeling consists in mathematically describing of the soil particle detachment, sediment transport and deposition on land surface (Lal, 1994). For assessing the soil erosion, many empirical models were developed in the past such as USLE, Universal Soil Loss Equation (Wischmeier & Smith, 1978); WEPP, Water Erosion Prediction Project (Nearing et al., 1989), EUROSEM, European Soil Erosion Model (Morgan et al., 1998) and many others (Pervoić et al., 2013). Among these known models, the USLE and revised RUSLE version are the most widely used models for assessing soil erosion hazard around the world, especially in the developing countries due to simplified structures and data demand. In recent years, the combined use of satellite imagery, geographic information system with RUSLE model makes soil erosion estimation on regional scale feasible with reasonable costs and better accuracy (Millward & Mersey, 1999; Wang et al., 2003; Lu et al., 2004; Jasrotia & Singh, 2006; Krishna Bahadur, 2009 in Prasannakumar et al., 2011). Many researchers applied USLE/RUSLE linked with remote sensing and GIS techniques for assessing soil erosion and sediments yields with successful results (Angima et al., 2003; Lee, 2004; Lu et al., 2004; Kim et al., 2005; Onyando et al., 2005; Onori et al., 2006; Pandey et al., 2007;

Erdogan et al., 2007; Ismail & Ravichandran, 2008; Yue-Qing et al., 2008; Ugur Ozcan et al., 2008; Krishna Bahadur, 2009; Terranova et al., 2009; Pandey et al., 2009; Arekhi et al., 2010; Jain & Das, 2010; Wang et al., 2010; Park et al., 2011; Chen et al., 2011; Kefi et al., 2011; Prasannakumar et al., 2012; Ozosy et al., 2012; Perović et al., 2012; Mhangara et al., 2012; Demirci & Karaburun 2012; Ashiagbor et al., 2013).

The quantity and quality of water and land available for agricultural production are two fundamental factors on which the economy of the country is mainly based. The selected area for this study, the northern part of Kirkuk Governorate, Iraq, is characterized by an abundance of fresh groundwater and arable land. Despite of the agricultural importance of the study area, and to the best knowledge of the authors, there are no studies concerning the spatial rate of soil erosion. This study integrates the empirical RUSLE model with remote sensing and GIS techniques to investigate the spatial distribution of annual soil loss potential in the northern Kirkuk Governorate, Iraq. Delineation of soil erosion zones is very important to protect soil and manage fertile land in a sustainable manner.

2. MATERIALS AND METHODS

2.1 Study area

The study area located in the northeast Kirkuk Governorate, north of Iraq, along the left side of Alton Kopri Basin between latitudes (35°30' – 35°51') and longitude (44°04' – 44°37') and occupies an area of 1,940 km^2 (Fig. 1).

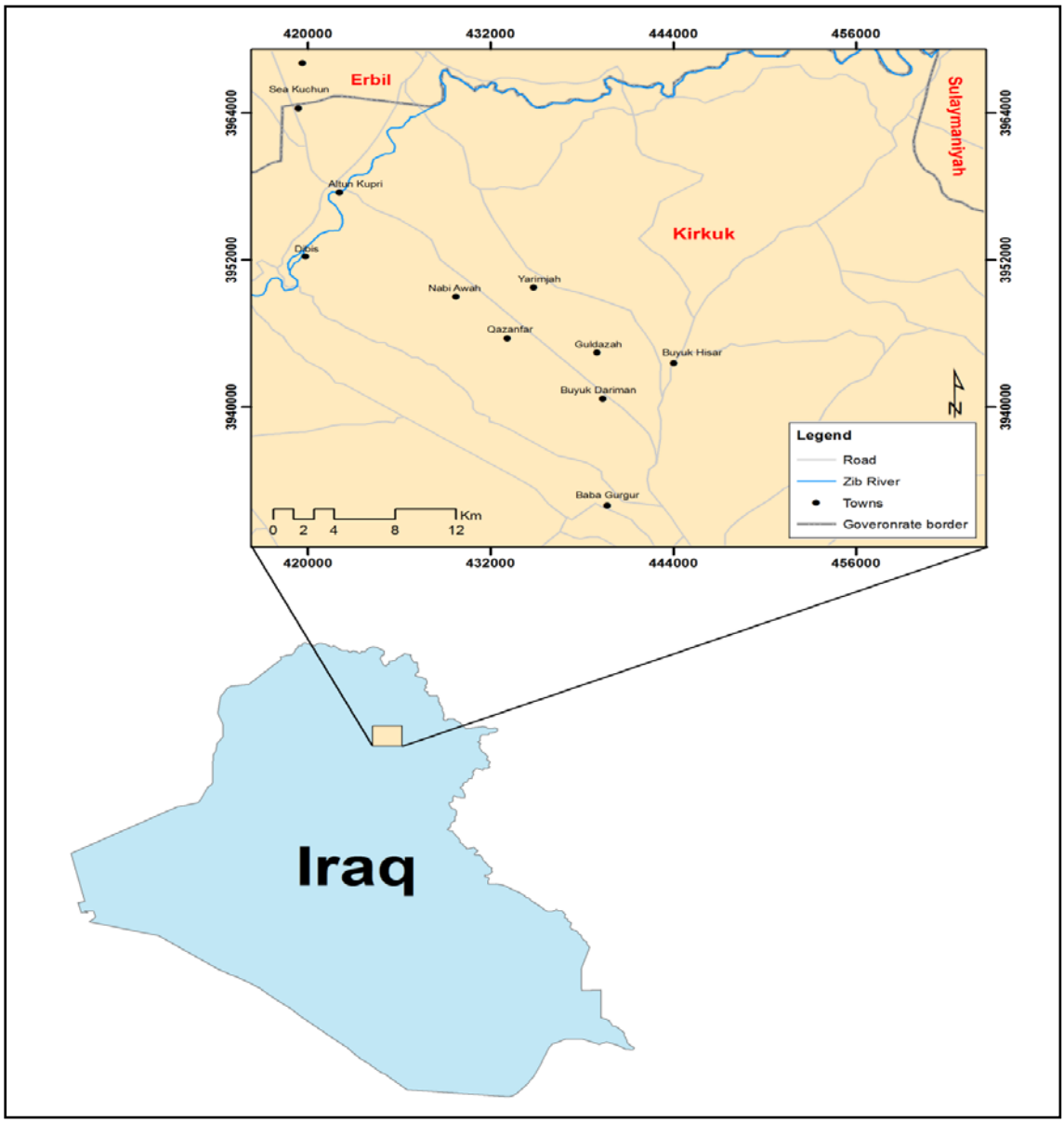

Figure 1. The northeast Kirkuk Governorate, along the left side of Alton Kopri Basin location in north of Iraq

The Lesser Zab River divides the whole area into two parts, right bank (northern part) belongs to Erbil Governorate, and left bank (southern part) lies in Kirkuk Governorate. The first series is represented by Kanydomlan which is considered a part of baba dome with a height of 450 m (msl) to the southwest of the area and the second is a series mountain (Kalkalan Dagh) with a height of about 800 m (msl) to the northeast of the study area. Generally, the region elevation ranges between 227 - 852 m above mean sea level (msl), (Fig. 2). The area shows symmetrical shape surrounded by two parallel chains of mountains. The first series is represented by Kanydomlan which is considered a part of Baba dome with height of 450 m (msl) to the southwest of the area. The second is a series mountain (Kalkalan Dagh) with height of about 800 m (msl) to the northeast of the study area. A small valley covered with silt and clay is permeating between these two chains (Al-Sayab et al., 1983). The southwest side of the area is particularly a very intense decline compared to the northeast side of the basin. The central area is almost a flat land with the interference of some bends and torsions due to the present of several simple wadis, which are filled with water through the seasonal rainfall and discharged toward the Julak valley. This is the main portion of the natural discharge to the Little Zab River (Al-Sayab et al., 1983).

The climate is hot and dry in summer, and cold, humid in winter. The rainy season is from October to May. The average annual precipitation is 342.7mmbut the evapotranspiration amounts 1662.9 mm. The dominant climate is semiarid.

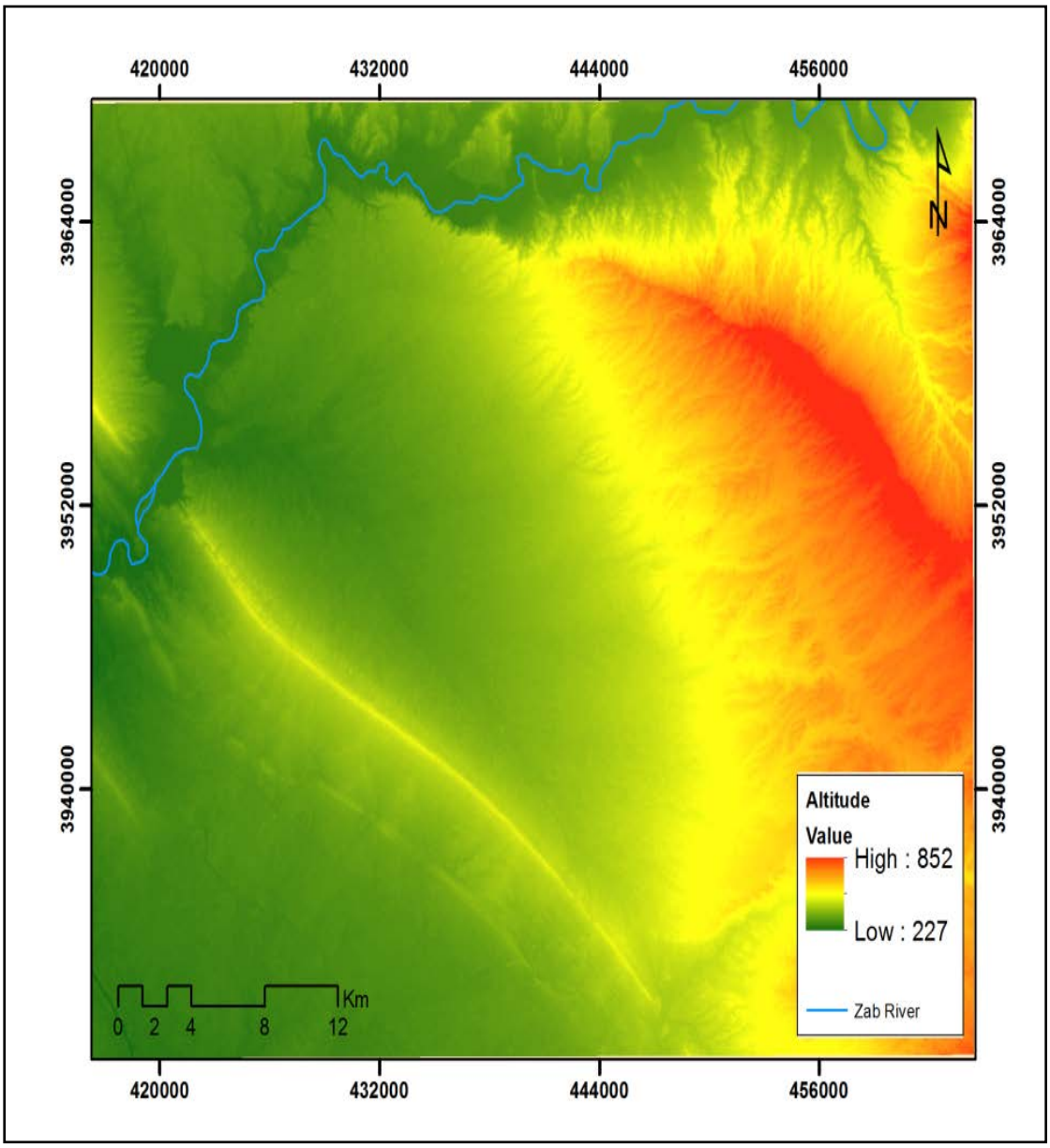

Figure 2. Spatial representation of elevation (m) in the study area

Four land use/land cover classes are prevailing in the study area, namely: herbaceous rangeland (1.5%), agricultural farms (10.2%), crop land (44.8%), barren land (32%), and urban (11.2%). The distinguished physiographic units in the area are high folded, foothill zone, flat, and river terraces (Haddad et al., 1971).

From a geological point of view, the study area is part of the foothill zone in the folded area of unstable shelf of Iraq. The unstable shelf had been most strong subsiding part of the Arabian plate since the opening of the southern neo- Tethys in the late Jurassic (Buday & Jassem, 1987). Maximum subsidence occurred during the late Cretaceous ophiolite obduction onto the NE margin of the Arabian Plate and during Mio-Pliocene continental collision. The unstable shelf is thus characterized by structural trend and facies changes that are parallel to the Zagros-Taurus suture belts. Surface folds are a characteristic feature of the unit. In the study area, outcrops formations are ranging in age between Miocene to Holocene. The Miocene formations are represented by Injana and Fatha Formations, consisting in clay layer. Pliocene layers occur in the Northeast of the basin and represented by Muqdadyi and Bi-Hassan Formations along Kalkalan Dagh series consisting of successive layers of gravel, conglomerate and thin red silty clayey seam. The Quaternary layers (loess, loess like deposits, alluvial) cover both the centre of the basin; called Julak Basinand the sides of the Little Zab Valley represented by fluvial terraces (Parson, 1955; Haddad et al., 1971).

The soil of the study area formed during the Quaternary period. Most of soils show brownish to yellow colour on top. According to Buringh (1960) there are four types of soil in the study area: lithosol soil with sandstone and gypsum, lithosol soil with limestone, moderately brown to shallow soils, and thick brown soils. The first type of soil was found in highland of Kirkuk and hills in northwest and west of Kirkuk city. These are often shallow and have been exposed, in places, to severe erosion to form water composed grooves as a result of rill erosion along the slopes. Buringh (1960) described them as poorly distributed, shallow in thickness at the highland slopes while the thickness increases at the foothills. The second type is brown in colour and is located within folded zones in areas of Bi- Hassan and Muqdadyi Formations. They are deposited at the foothills of Kalkalan Dagh mountain series in the north east of the area). Generally, the soils of this area are shallow and do not exceed 30 cm in thickness. They are Aluviosoils, mixed with gravels and accumulated limestone separate between them. They are proper for grazing, when small little grass spreads in the area (Buringh, 1960). The third type of soils extends in the folded zone within the hills where the deep valleys descend spreading from the hills. These are shallow to moderate soils. They are environmentally classified as grasslands being suitable for grazing (Buringh, 1960). The fourth type is represented by brown lithosol soils with moderate to deep thickness. They occur both in the eastern and western side of Kanydomlan Mountain series an in the centre of the basin. These soils are likely to be formed from wind erosion, river sediment transport and deposition. They consist of alluvial clay, silt and sand, and also contain a small amount of gypsum especially near the Kanydomlain Mountain. They are considered to be a good area for the cultivation of winter crops depending on rainfall availability (Buringh, 1960).

2.2. Methods

The RULSE has been widely used to predict the average annual soil loss by introducing improved means of computing the soil erosion factors. Basically, the magnitude of soil erosion depends on two factors, namely: the detachment of soil particles by the impact of rainfall energy, called the erosivity of rain, and the ability of the soil to resist the detachment of its particles by this force, called the erodibility of soil (Wischmeier & Smith, 1960 and 1978). The RULSE equation states that: (Wischmeier & Smith, 1978; Renard et al., 1997)

$$A = R \times K \times LS \times C \times L \qquad (1)$$

where A is the annual average of soil erosion rate factor [t ha^{-1} yr^{-1}]; R is the rainfall erosivity factor [MJ mm ha^{-1} h^{-1} yr^{-1}]; K is the soil erodibility factor [t ha^{-1} h-1 MJ mm^{-1}); LS is the slope – steepness factor (dimensionless); C is the crop management factor (dimensionless, ranging between 0 and 1); and P is the conservation support practice (dimensionless, ranging between 0 and 1). The erosivity of rain is represented by the factor R, and the erodibility of the soil surface system by the multiples of factors KLSCP.

For this study, the RULSE five factors were prepared by means of ArcGIS 10.2 commercial software. Input five factors belongs to monthly and annual rainfall data, soil data, digital elevation model, and satellite imagery were acquired from different resources such as Iraqi Meteorological Commission archives, field surveys, and web resources for DEM and LANDSAT 8 images. All five factors were prepared as raster from with 30m × 30m cell size in spatial analysis extension of ArcGIS software. The projected coordinate system for all thematic layers was (UTM WGS 1984- 38N).

3. GENERATING OF RULSE THEMATIC LAYER FACTORS

3.1 Rainfall erositivity (R factor)

The rainfall erosivity (R) factor is defined as the potential ability of rain to cause erosion and given as the product of a given rainfall storms' maximum 30-min intensities (I30) and the kinetic energy of rainstorm (E) (Wischmeier & Smith, 1958, 1960 and 1978). The calculated erosion potential of rainfall storm is usually written as EI30. The total R is therefore the sum of individual EI30 values for each rainfall storm event. Unfortunately, these measurements are rarely available at standard meteorological stations in Iraq. The alternative practical option is by using monthly and annual rainfall data collected from a single weather station (Wischmeier & Smith, 1958, 1978; Arnoldus, 1980):

$$R = \sum_{i=1}^{12} 1.735 \times 10^{\left(1.5 \times \log_{10}\left(\frac{P_i^2}{P}\right) - 0.08188\right)} \qquad (2)$$

where R is the rainfall erosivity (MJ mm ha^{-1} h^{-1} yr^{-1}), Pi is the monthly rainfall (mm), and P is the annual rainfall total (mm). Since there is no any meteorological station in the study area, data from the following nearby stations were used for estimating R values: Erbil, Sulaymaniyah in Iraqi Kurdistan region, Kirkuk and Baiji. Table 1 shows the estimated R values along with other relevant information. The R values ranges between 108.26 - 716.28 with average value of 368.40 (MJ mm ha^{-1} h^{-1} yr^{-1}). It is obvious from table 1 that the calculated R is directly related with annual rainfall; high rainfall leads to high R values, and vice versa. The spatial interpolation of R is impossible with only four values or could be interpolated but with large errors. Therefore, the average value of R was assumed to be uniform over the study area and was used for the subsequent analysis.

3.2 Soil erodibility (K factor)

The K factor is the product of susceptibility of soil particles to erosion per unit of rain erosivity factor (R), for a specified soil on a unit plot having a 90% uniform slope and a slope length of 22.13 m over a continuously clean shallow land with up and down slope farming (Wischmeier & Smith, 1960 and 1978).

Table 1. Calculated rainfall erosivity factor R from monthly and annual rainfall for considered stations

Meteorological station	Location (UTM)		average of monthly rainfall (mm)						annual rainfall (mm)	rainfall erosivity (MJ mm ha-1 h-1 year-1)
Erbil	410274.86	4005904.21	Jan	Feb	Mar	Apr	May	Jun	241.22	387.83
			74.5	74.4	75.2	54.7	11.9	1.3		
			Jul	Aug	Sep	Oct	Nov	Dec		
			0.5	0.1	0.7	30.8	52.1	80.3		
Sulaymaniyah	539259.49	3934466.56	Jan	Feb	Mar	Apr	May	Jun	449.78	716.28
			122	110	107	87.2	39.7	1.9		
			Jul	Aug	Sep	Oct	Nov	Dec		
			0.0	0	1.4	33.2	96.5	118		
Kirkuk	444670.76	3925206.21	Jan	Feb	Mar	Apr	May	Jun	181.21	261.23
			68.7	66.8	50	43.5	13.8	0.2		
			Jul	Aug	Sep	Oct	Nov	Dec		
			0.3	0.1	1	14.7	45.6	56.9		
Baiji	361326.84	3865674.76	Jan	Feb	Mar	Apr	May	Jun	72.42	108.26
			36.2	35.8	30.5	20	11.5	0.5		
			Jul	Aug	Sep	Oct	Nov	Dec		
			0.0	0	1	8.9	26.9	29.8		

Table 2 Soil structure degree criteria (Chen et al., 2011)

a (%)	≤ 0.5	0.5- 1.5	1.51-4.0	≥ 4.0
Soil structure code b	1	2	3	4

Table 3 Soil permeability degree criteria (Chen et al., 2011)

Clay %	≤ 10	10- 15.9	16-21.6	21.7-27.4	27.5-39	≥ 39.1
Soil permeability code b	1	2	3	4	5	6

It reflects the ease with which the soil is detached by splash during rainfall and/ or surface flow (Dumas et al., 2010). The K factor is closely related to soil texture (percent of clay, silt, and sand), organic matter content (%), soil texture and soil permeability. The K factor for the study area was estimated by using the following equation (Wishmeier & Smith, 1978; Foster et al., 1980)

$$K = 2.8\times10^{-7} M^{1.14}(12-a) + 4.3\times10^{-3}(b-2) + 3.3\times10^{-3}(c-3) \quad (3)$$

where M is the particle size parameter (% silt + % very fine sand) (100 - % clay); a is organic content of soil %; b is the soil structure code (Table 2); c is the profile permeability class (Table 3).

For calculating K (t ha^{-1} h^{-1} MJ mm^{-1}), a total of 22 samples of soil were collected at a depth of about 50 cm below the surface after removing the top soil cover. The soil samples were collected in clean polyethylene containers and transported to soil laboratory of Civil Engineering/ Engineering College/University of Basra to carry out grain size analysis. Locations of these samples were selected after many criteria, such as easiness to access, even distribution over the study area, and ease to dig through the soil surface. The collected soil samples were assigned texture names based on the web-based USDA soil texture calculator. Organic matter content was measured by using analytical technique. Four soil textures were found in the study area, namely: sandy loam, loam, sandy clayey loam, and loamy sand (Table 4). The most dominant soil texture was sandy loam. The K values were then calculated using eq. 3 and interpolated using weighted inverse distance deterministic interpolation method to create thematic layer raster (Fig. 3). The calculated K values were in range 0.04 to 0.38 with K average equals to 0.14.

3.3 Slope-Steepness (LS) factor

The LS factor represents erodibility due to combinations of slope length and steepness relative to a standard unit plot (Wischmeier & Smith, 1960 and 1978; Ashiagbor et al., 2013). Slope length (L) is defined as the horizontal distance from the point of origin of the overland flow to the point where either the slope gradient decreases enough that deposition begins or runoff is concentrated in a defined channel (Wischmeier & Smith, 1978 in Ozosy et al., 2012). On the other hand, the influence of slope gradient on soil erosion could be described by slope steepness (S) factor. An increase in slope length and steepness causes an increase in the LS factor. For estimation of the LS factor, the following relationship was adapted: (Jain & Das, 2010).

$$LS = \left[\frac{A_s}{22.12}\right]^n \left[\frac{\sin\beta}{0.0896}\right]^m \quad (4)$$

where A_s is the specific area (A/b), defined as the upslope contributing area for overland grid (A)

Table 4. The calculated soil erodibility (K) values for the soil samples

Sample No.	Easting	Northing	Soil texture	K (t ha h ha^{-1} MJ mm^{-1})
S1	442815	3936960	Sandy loam	0.13
S2	436742	3943197	Sandy loam	0.13
S3	424462	3951489	Loam	0.38
S4	421648	3957213	Sandy loam	0.13
S5	425314	3957151	Sandy clay loam	0.2
S6	443813	3943612	Sandy loam	0.13
S7	446972	3937708	Sandy loam	0.13
S8	453022	3934686	Loamy sand	0.04
S9	453470	3943402	Loamy sand	0.04
S10	445277	3948471	Loam	0.38
S11	442713	3952430	Sandy loam	0.13
S12	440817	3950748	Sandy loam	0.13
S13	434243	3952089	Sandy loam	0.13
S14	431197	3957904	Sandy loam	0.13
S15	440357	3964462	Sandy loam	0.13
S16	444025	3965270	Loam	0.38
S17	427326	3957442	Loamy sand	0.04
S18	428102	3963382	Sandy loam	0.13
S19	447587	3956621	Sandy loam	0.13
S20	445588	3958297	Sandy loam	0.13
S21	428027	3957251	Sandy loam	0.13
S22	431236	3946750	Loamy sand	0.04

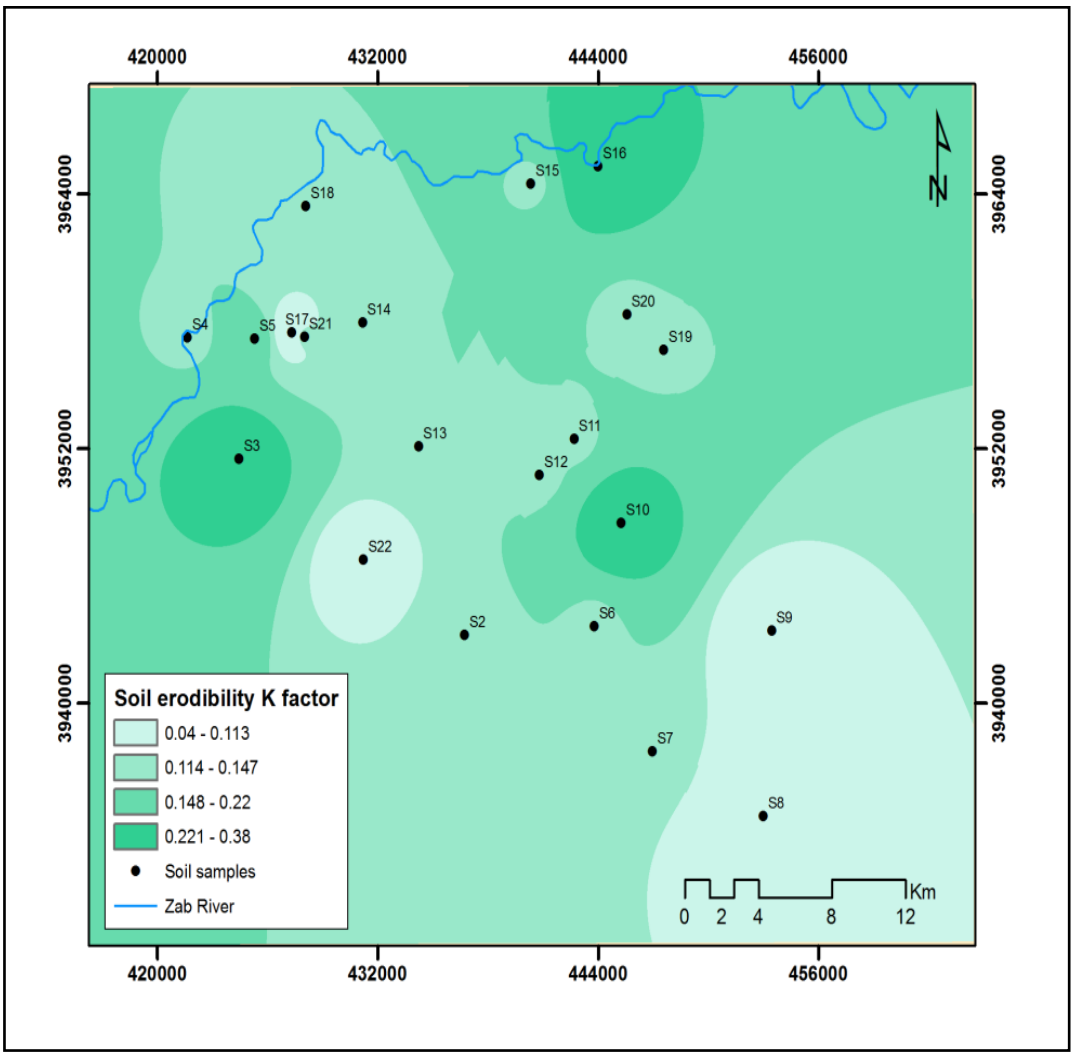

Figure 3. Spatial distribution of soil erodibility factor (K), for the studied area

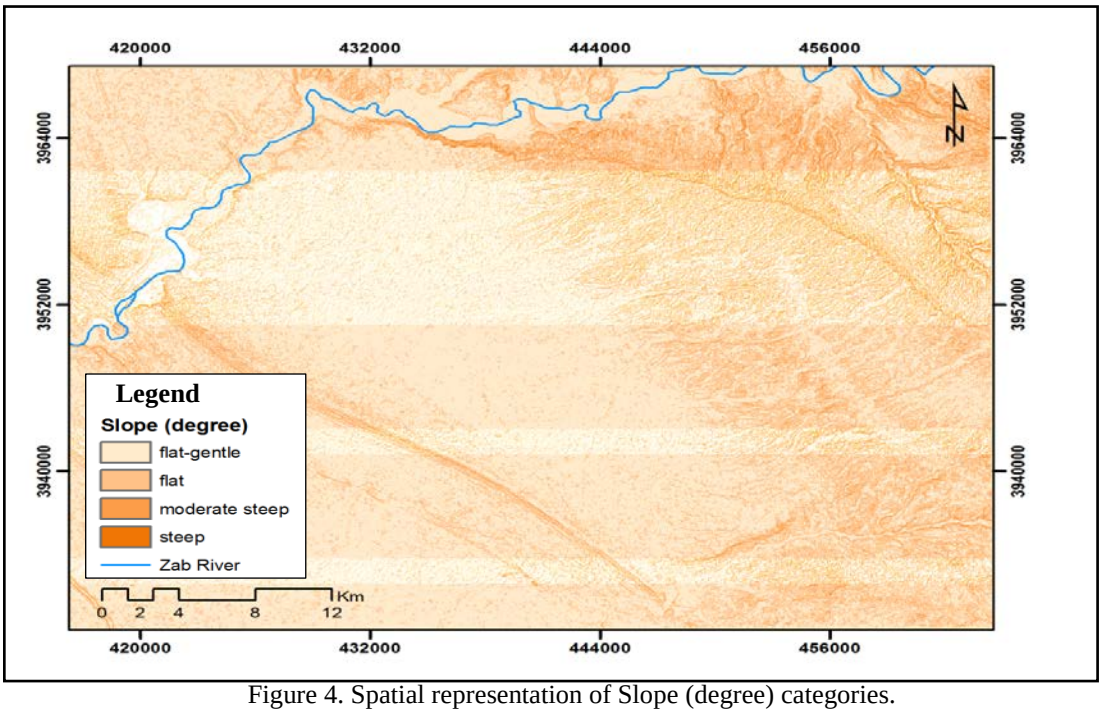

Figure 4. Spatial representation of Slope (degree) categories.

per unit width normal to flow direction (b); β is the slope gradient in degree; n and m are constants, usually taken as 0.4 and 1.3 for n and m, respectively (Lee, 2004).

For this study, the LS factor was estimated from the Advanced Spaceborne Thermal Emission and Reflection Radiometer (ASTER) Global Digital Elevation Model(GDEM) The ASTER-GDEM was developed by the Ministry of Economy of Japan and the United States National Aeronautics and Space Administration (NASA). The spatial resolution of the ASTER-GDEM is approximately 30 m. The eq. 2 can be written from hydrological parameters derives from DEM as:

$$LS = Power(Flow\,accumulation \times cell\,size/22.13, 0.4) \times \times Power(\sin(slope)/0.0896, 1.4) \quad (5)$$

The original ASTER-GDEM was firstly re-projected to (UTM WGS 1984 38N) projected coordinate system, clipped for the study area, reconditioning, and fill sinks. The flow direction and flow accumulation layers were derived from filled ASTER-GDEM by using the Arc Hydro extension in ArcGIS 10.2. The slope layer was derived from filled DEM using spatial analyst extension (Fig. 4). The minimum, maximum, and mean of slope (degree) were 0, 44.3, and 4.6, respectively. The slope raster layer was classified into four categories: gentle flat, flat, moderately steep and steep (Pourghasemi et al., 2013). The relative area (%) covered by each of these categories were 65.8%, 31.2%, 3%, and 0.1%, respectively.

The extent of gentle-flat and flat categories ≈ 79% mean that affecting of this factor on soil loss is fairly small. The raster calculator of ArcGIS 10.2 was used to calculate LS using eq. 4 to derive the thematic layer of LS of the study area (Fig. 5). The range of LS factor is from 0 to 10.76 with an average value of 0.02.

3.4 Crop management (C) factor

The C factor is defined as the ratio of soil loss from land cropped under specified conditions to the corresponding loss from clean-tilled, continuous, fallow land (Wischmeier & Smith, 1960 and 1978; Das, 2002). It reflects the effect of cropping and management practices on soil erosion rate (Renard et al., 1997). The easiest way for calculating C factor is through using remote sensing data. The Normalized Difference Vegetation Index (NDVI) is normally used for estimating C factor through the following formula: (Zhou et al., 2008; Kouli et al., 2009; Prasannakumar et al., 2012)

$$C = \exp\left[-\alpha \frac{NDVI}{(\beta - NDVI)}\right] \quad (6)$$

where α and β are unitless parameters that determine the shape of the curve relating to NDVI and the C-factor and usually taken as 2 and 1 for α and β, respectively (Van der Knijff et al., 2000; Perović et al., 2012). NDVI is one of the different indices developed to identify vegetated areas and their "condition" and it remains the most well-known and used index to detect live green plant canopies in multispectral remote sensing data. The NDVI is calculated as follows:

$$NDVI = \frac{(NIR - VIS)}{(NIR + VIS)} \quad (7)$$

where NIR and VIS are the spectral reflectance measurements acquired in the visible (red) and near-infrared regions, respectively.

For this study, LANDSAT 8 multiband image acquired in 26/5/2014 was used for calculating C factor. The image was downloaded from USGS web location (http://earthexplorer.usgs.gov/). The bands were composed together to create composed image, clipping for the study area, radiometric enhancement, and then the NDVI was automatically calculated using Image analysis extension in ArcMap. Eq. 7 then used for estimating C factor and is presented graphically as a raster thematic layer in (Fig. 6). The minimum, maximum, and mean values of C were 0.38, 0.76, and 0.55, respectively.

3.5 Practice Management (P) factor

The P factor is the ratio of soil loss with a specific support practice to the corresponding soil loss with up and down cultivation (Wishmeier & Smith, 1960 and 1978). The lower P value, the more effective the conservation practice, is deemed to be at reducing soil erosion (Lee, 2004). The numerical value of P is always less than 1. The P value is 1 if there is no management practice. The P factor value is taken as 1 for the whole study area because no data available concerning the management practice for the concerning area.

4. RESULTS AND DISCUSSION

The annual soil loss was estimated by equation (1) implemented in raster calculator of spatial analyst extension and presents graphically in (Fig. 7). The annual soil loss rate estimated for the study area ranges from 0 to 245 (t ha^{-1} yr^{-1}). There is no Iraqi standard for the classification of this range. Therefore, four classification schema were used for comparing results, namely: natural breaks, quantile, geometric, and

standard deviation. The detailed description of these schema was found with ArcGIS help (ESRI, 1999). The soil potential values were grouped into four categories: minimal, low, moderate, and high using those different classification schemas.

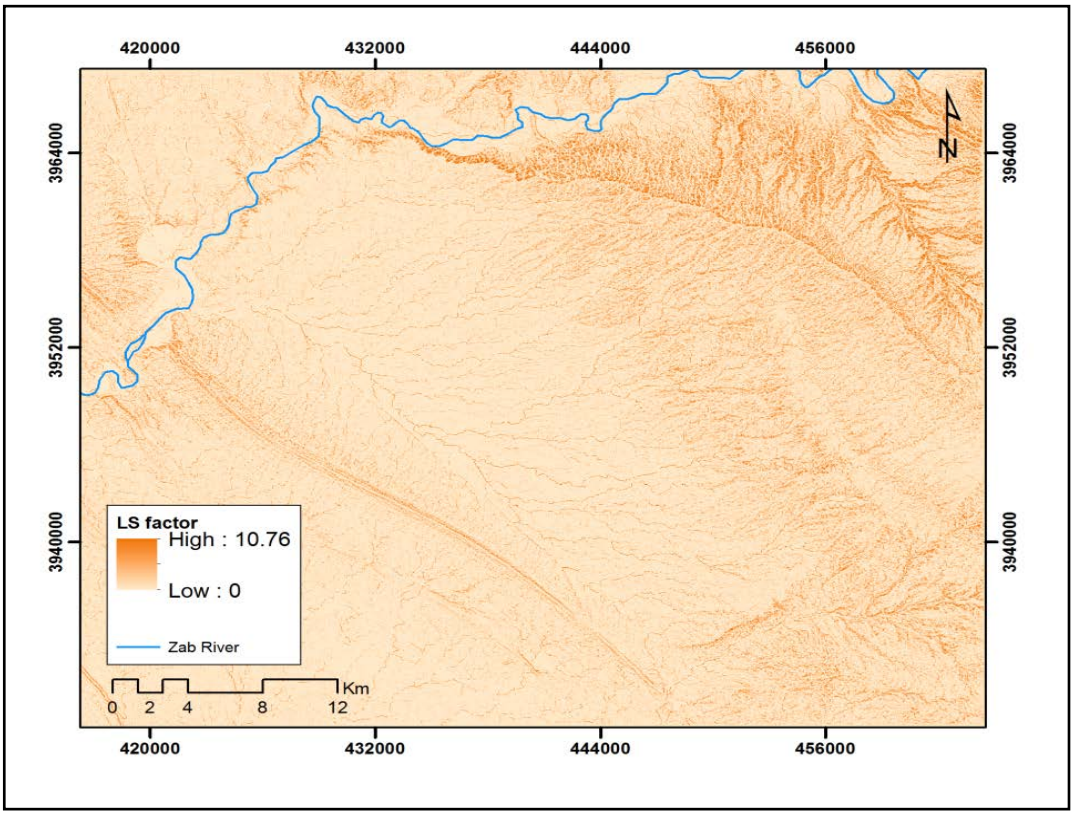

Figure 5. Spatial distribution of LS factor (dimensionless)

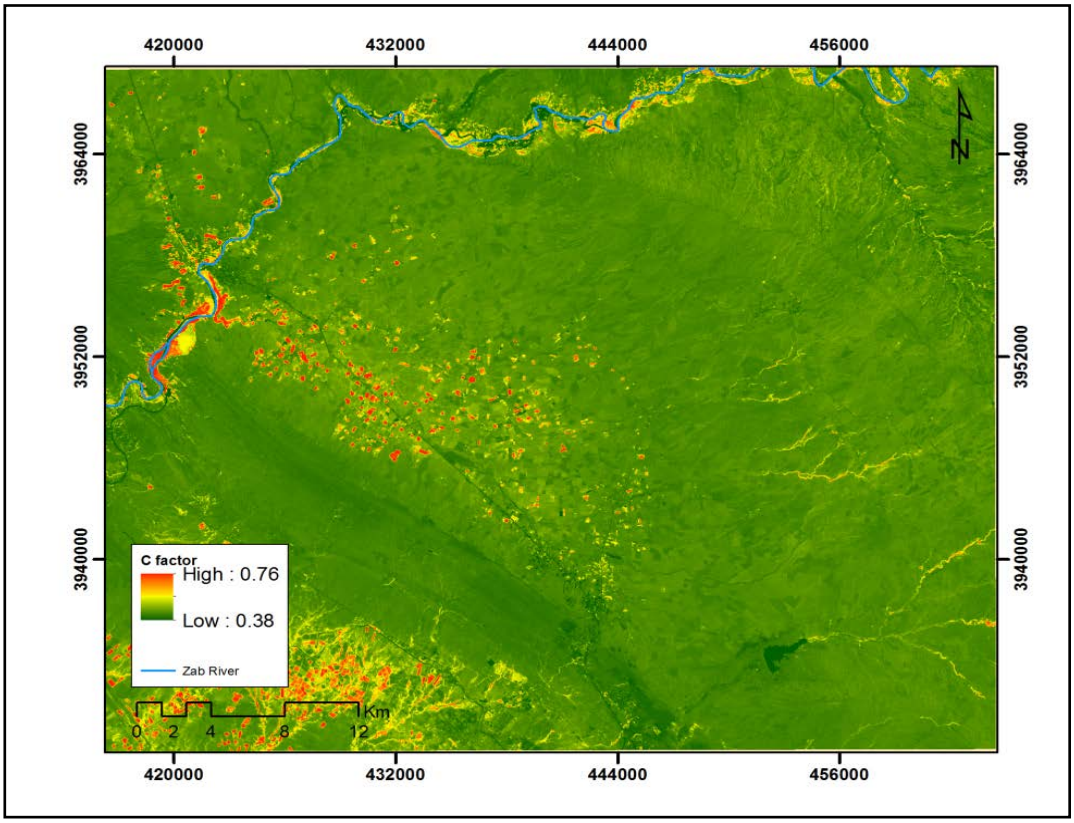

Figure 6. Spatial distribution of C factor as a raster thematic layer

Table 5 shows that it is difficult to choose which classification scheme fits best for the study area, but in general, the geometric and quantile approximately have the same results if compared with natural breaks and standard deviation schema which also have the same figures. Therefore, the comparison was done only by using two schemas: the geometric and natural breaks, (Fig. 8). The obtained results presented in table 5 were also further reduced into two categories to facilitate comparing the process (Table 6). This table also contains a correlation between slope categories and soil hazard risk zones. The area covered by minimal-low soil hazard zones extend over an relative area of about 88% and 99% based on geometric and natural breaks schema, respectively.

The moderate-high soil hazard zones cover only very small area (0.3%) based on natural breaks and relatively small area (12%) depending on geometric scheme. In general, the results obtained through both methods indicate that hazard of soil erosion in the study area is low.

The spatial pattern of classified soil erosion rate indicates that the areas with moderate to high risks are located in the northeast and just a few in the east, while the minimal to low zones comprises other parts of the study area. From tables 4 and 5 it is obvious that there is very strong relationship between slope and soil loss categories.

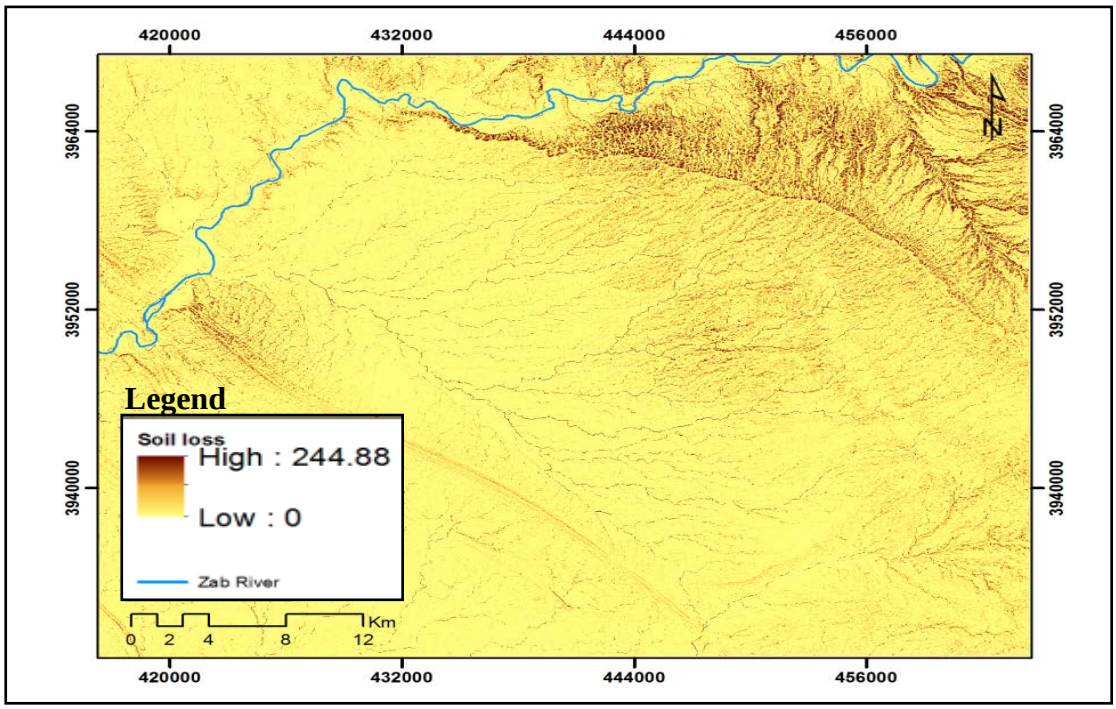

Figure 7. Spatial distribution of annual soil erosion (t ha^{-1} yr^{-1}), the annual soil loss rate estimated for the study area ranges from 0 to 245 (t ha^{-1} yr^{-1}).

Table 5. Comparison of calculated soil loss using four different classification schemes

Soil risk	Geometric		Quintile		Natural breaks		Standard deviation	
	Pixels	%	Pixels	%	Pixels	%	Pixels	%
Minimal	1147762	0.530	1038949	0.480	2045609	0.944	1904913	0.879
Low	761225	0.351	864820	0.399	115170	0.053	168769	0.078
Moderate	255036	0.118	194906	0.090	5425	0.003	47764	0.022
High	2454	0.001	67802	0.031	273	0.000	45031	0.021

Table 6. The relation between slope and soil erosion categories

Slope categories	%	Soil risk	Geometric	Natural breaks
gentle flat - flat	0.970	minimal-low	0.881	0.997
moderately steep-steep	0.031	moderate-high	0.119	0.003

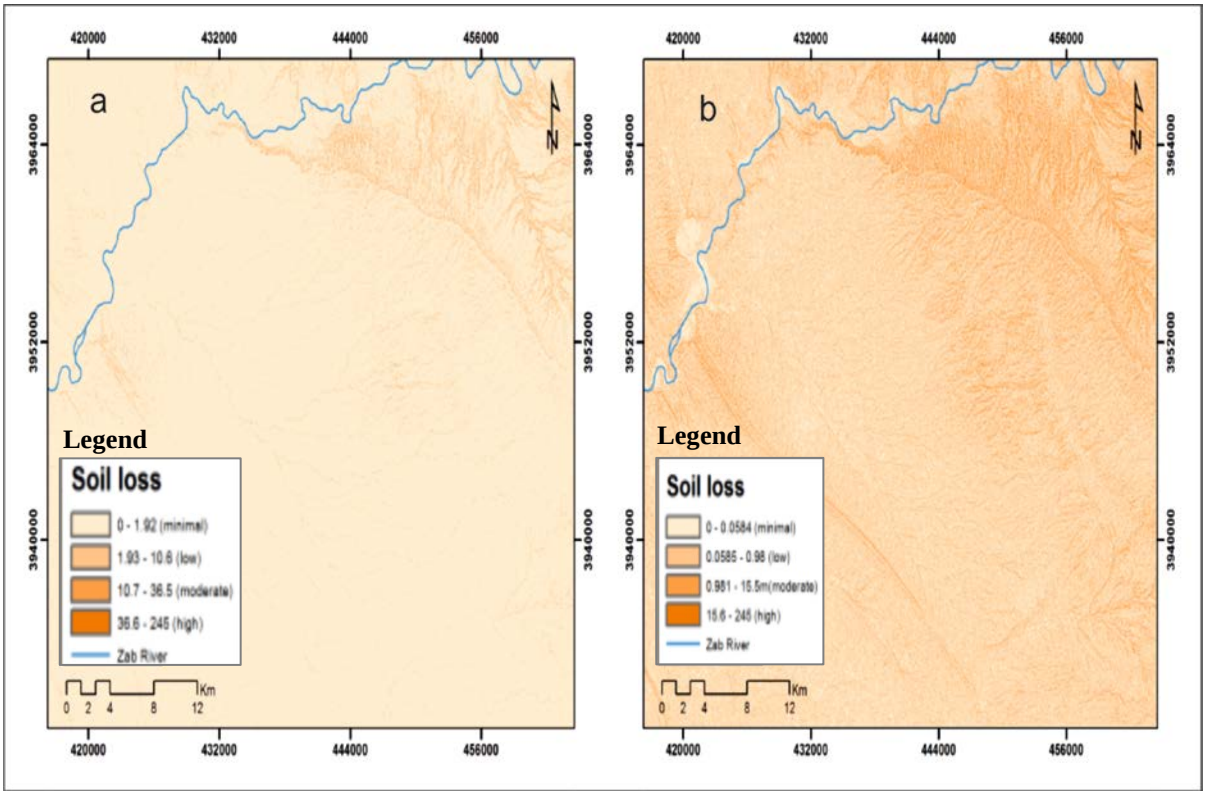

Figure 8. Comparison between (a) natural breaks and (b) geometric classification schema for soil loss hazard zones identification.

5. CONCLUSIONS

The main objective of this study was to assess the spatial distribution of annual soil loss over the northern part of Kirkuk Governorate, Iraq using RULSE model. The five factors of RULSE were derived from different resources. The R factor was estimated from annual and monthly rainfall data of meteorological stations close and around the study area. The calculated R values range from 108.26 to 716.28 with average value of 368.40 (MJ mm ha^{-1} h^{-1} yr^{-1}).

The K factor was estimated from collected soil samples and the calculated K values vary from 0.04 to 0.38 with an average of 0.14 (t ha^{-1} h^{-1} MJ mm^{-1}). The topographic factor (LS) was estimated from DEM with 30 m resolution. The range of LS factor was from 0 to 10.76 with an average value of 0.02. The C factor was estimated from remote sensing data and by using Normalized Difference Vegetation Index (NDVI). Minimum, maximum, and mean values of estimated C were 0.38, 0.76, and 0.55, respectively. The P factor was assumed to be one because there is no apparent practice management in the study area. The map of spatial distribution of soil loss revealed that the average of soil loss was found between 0 - 245 (t ha^{-1} yr^{-1}) with an average of 2 (t ha^{-1} yr^{-1}). The soil erosion values were classified into four soil erosion hazard zones: minimal, low, high, and very high by using different classification schema. The area covered by minimal-low soil hazard zones covers a relative area of 88% - 99% based on geometric and natural breaks schemes, respectively .In turn, the moderate-high soil hazard zones only cover very small area (0.3%) based on natural breaks and relatively small area (12%) depending on geometric scheme. The areas at moderate to high risk are found primarily in the north-eastern part of the study area and strongly related with slope. Soil conservation practices have to be implemented to reduce soil erosion. Generally, the obtained results indicate that hazard of soil erosion in the study area is low. To get more accurate soil erosion status in the study area, it is recommended to derive land use/land cover map and relate it to soil erosion map.

REFERENCES

Al-Sayab A.A., Hassan H.A., Ayob M.S., Taha S.H., Salih A.Y. & Faizi K.N., 1983. Water- salt balance and supplementary irrigation of Alton Copry Basin, Tech Rep No 14811 SRC. 89p.

Angima S.D., Stott D.E., O'Neill M.K., Ong C.K. & Weesies G.A., 2003. Soil erosion prediction using RUSLE for Central Kenyan highland conditions. Agric Ecosyst Environ 97(1–3):295–308.

Arekhi S., Niazi Y. & Kalteh A., 2010. Soil erosion and sediment yield modeling using RS and GIS techniques: a case study, Iran. Arab J Geosci. 5(2): 285-297. doi: 10.1007/s12517-010-0220-4.

Arnoldus H.M.J., 1980. An approximation of the rainfall factor in the universal soil loss equation. In: De Boodt M, Gabriels D (eds) Assessment of erosion. Wiley, Chichester, pp 127–132.

Ashiagbor G., Forkuo E.K., Laari P. & Aabeyir R., 2013. Modeling soil erosion using RUSLE and GIS tools. International journal of remote sensing & geosciences 2(4): 7-17.

Buday T. & Jassim S.Z., 1987. The Regional Geology of Iraq, Vol.2: Tectonism, Magmatism, and Metamorphism. GEOSURV, Baghdad, 352 p.

Buringh D.P., 1960. Soils and Soil Condition of Iraq. Ministry of Agriculture, Baghdad, Iraq, 337 p.

Chen T., Niu R., Wang Y., Li P., Zhang L. & Du B., 2011. Assessment of spatial distribution of soil loss over the upper basin of Miyun reservoir in China based on RS and GIS techniques. Environ Monit Assess 179:605–617. doi: 10.1007/s10661-010-1766-z.

Das G., 2002. Hydrology and soil conservation engineering. Prentic-Hall of India, 459 p.

Demirci A. & Karaburun A., 2012. Estimation of soil erosion using RUSLE in a GIS framework: a case study in the Buyukcekmece Lake watershed, northwest Turkey. Environ Earth Sci 66:903–913. doi: 10.1007/s12665-011-1300-9.

Dumas P., Printemps J., Mangeas M. & Luneau G., 2010. Developing erosion models for integrated coastal zone management: a case study of the new Caledonia West Coast. Marine Pollution Bull 61(7): 519-529.

Erdogan E.H., Erpul G & Bayramin İ., 2007. Use of USLE/GIS methodology for predicting soil loss in a semiarid agricultural watershed. Environ Monit Assess 131:153–161. doi: 10.1007/s10661-006-9464-6.

ESRI., 1999. Getting started with ArcGIS. USA. 260p.

Foster G.R., Lane L.J., Nowlin J.D., Laflen J.M. & Young R.A., 1980. A model to estimate sediment yield from field-sized areas: development of model. In: Knisel WG (ed) CREAMS: a field scale model for chemicals, runoff, and erosion from Agricultural Management Systems, US Dept. of Agric., Sci. and Educ. Admin., Conser. Rep. No. 26, pp 36–64.

Haddad H.R., Al-Jawad S.B., Haddad I., Younan A.I., Salvo A.V., 1971. Hydrogeological investigation in Jolak Basin of the Alton Copry area. Tech Rep No 25 Institute for Applied Research on Natural Resources, 38p.

Ismail J. & Ravichandran S., 2008. RULSE2 model application for soil erosion assessment using remote sensing and GIS. Water Resour Manage (2008) 22:83–102. doi: 10.1007/s11269-006-9145-9.

Jain M.K. & Das D., 2010. Estimation of sediment yield and areas of soil erosion and deposition for watershed prioritization using GIS and remote sensing. Water Resour Manage 24:2091–2112. doi: 10.1007/s11269-009-9540-0.

Jasrotia A.S. & Singh R., 2006. Modeling runoff and soil erosion in a catchment area, using the GIS, in the Himalayan region, India. Environ Geol 51:29–37.

Kefi M., Yoshino K. & Setiawan Y., 2011. Assessment and mapping of soil erosion risk by water in Tunisia using time series MODIS data. Paddy Water Environ. 10(1): 59-73. doi: 10.1007/s10333-011-0265-3.

Kim J., Saunders P. & Finn J., 2005. Rapid assessment of soil erosion in the Rio Lempa basin, central America, using the universal soil loss equation and GIS. Environ Manage 36: 872–885. doi: 10.1007/s00267-002-0065-z.

Kouli M., Sopios P. & Vallianatos F., 2009. Soil erosion prediction using the Revised Universal Soil Loss Equation (RUSLE) in a GIS framework, Chania, Northwestern Crete, Greece. Environ Geol 57:483–497.

Krishna Bahadur K.C., 2009. Mapping soil erosion susceptibility using remote sensing and GIS: a case of the upper Nam Wa watershed, Nan Province, Thailand. Environ Geol 57:695–705. doi: 10.1007/s00254-008-1348-3.

Lal R., 1994. Water management in various crop production systems related to soil tillage. Soil Tillage Res 30: 169-185.

Lee S., 2004. Soil erosion assessment and its verification using the universal soil loss equation and geographic information system: a case study at Boun, Korea. Environ Geol 45:457–465. doi: 10.1007/s00254-003-0897-8.

Lu D., Li G., Valladares G.S. & Batistella M., 2004. Mapping soil erosion risk in Rondonia, Brazilian Amazonia: using RUSLE, remote sensing and GIS. Land Degrad Dev 15:499–512.

Mhangara P., Kakembo V. & Lim K., 2012. Soil erosion risk assessment of the Keiskamma catchment, South Africa using GIS and remote sensing. Environ Earth Sci 65:2087–2102. doi: 10.1007/ s12665-011-1190-x.

Millward A.A. & Mersey J.E., 1999. Adapting the RUSLE to model soil erosion potential in a mountainous tropical watershed. Catena 38(2):109–129. doi:10.1016/S0341-8162(99)00067-3.

Morgan R.P..C, Quinton J.N., Smith R.E., Govers G., Poesen J.W.A., Auerswald K., Chisci G., Torri D. & Styczen M.E., 1998. The European soil erosion model (EUROSEM): a dynamic approach for predicting sediment transport from fields and small catchments. Earth Surf Proc Land 23:527–544. doi:10.1002/(SICI) 1096-9837(199806).

Nearing M.A., Foster G.R., Lane L.J. & Finkner S.C., 1989. A process based soil erosion model for USDA-water erosion prediction project technology. T ASAE 32(5): 1587–1593.

Onori F., De Bonis P. & Grauso S., 2006. Soil erosion prediction at the basin scale using the revised universal soil loss equation (RULSE in a catchment of Sicily (southern Italy). Environ Geol 50: 1129–1140. doi: 10.1007/s00254-006-0286-1.

Onyando J.O., Kisoyan P. & Chemelil M.C., 2005. Estimation of potential soil erosion for River Perkerra catchment in Kenya. Water Resour Manage 19: 133–143. doi: 10.1007/s11269-005-2706-5.

Ozosy G., Aksoy E., Sabri Dirim M. & Tumsavas Z., 2012. Determination of soil erosion risk in the Mustafakemalpasa river basin, Turkey, using the revised universal soil loss equation, geographic information system, and remote sensing. Environ Manage 50:679–694. doi: 10.1007/s00267-012-9904-8.

Pandey A., Chowdary V. & Mal B., 2007. Identification of critical erosion prone areas in the small agricultural watershed using USLE, GIS and remote sensing. Water Resour Manage (2007) 21:729–746. doi: 10.1007/s11269-006-9061-z.

Pandey A., Mathur A., Mishra S. & Mal B., 2009. Soil erosion modeling of a Himalayan watershed using RS and GIS. Environ Earth Sci (2009) 59:399–410. doi: 10.1007/s12665-009-0038-0.

Park S., Oh C., Jeon S., Jung H. & Choi C., 2011. Soil erosion rick in Korean watersheds, assessed using the revised universal soil loss equation. J Hydrol 399: 263–27.

Parson R.M., 1955. Groundwater resource of Iraq, vol.4 Kirkuk Liwa. Development Board, Ministry of Development, Government of Iraq, 142 p.

Perović V., Životić L., Kadović R., Đorđević A., Jaramaz D., Mrvić V. & Todorovic M., 2012. Spatial modeling of soil erosion potential in a mountainous watershed of south-eastern Serbia. Environ Earth Sci 68: 115-128. doi: 0.1007/s12665-012-1720-1.

Pourghasemi H.R., Pradhan B., Gokceoglu C. & Moezzi KD., 2013. A comparative assessment of prediction capabilities of Dempster-Shafer and weights-of-evidence models in landslide susceptibility mapping using GIS. Geomatics, Nat Hazards and Risk 4(2): 93-118.

Prasannakumar V., Shiny R., Geetha N. & Vijith H., 2011. Spatial prediction of soil erosion risk by remote sensing, GIS, RULSE approach: a case study of Siruvani river watershed in Attapady valley, Kerala, India. Environ Earth Sci (2011) 64:965–972. doi: 10.1007/s12665-011-0913-3.

Prasannakumar V., Vijith H., Abinod S. & Geetha N., 2012. Estimation of soil erosion risk within a small mountains sub-watershed in Kerala, India, using revised universal loss equation (RULSE) and geo-information technology. Geoscience Frontier 3(2): 209-215.

Renard K.G., Foster G.R., Weesies G.A., McCool D.K. & Yoder D.C., 1997. Predicting Soil Erosion by Water: A Guide to Conservation Planning with the Revised Universal Soil Loss Equation (RUSLE). US Department of Agriculture, Agriculture Handbook No. 703: 404 pp.

Terranova O., Antronico L., Coscarelli R .& Iaquinta., 2009. Soil erosion risk scenarios in the Mediterranean environment using RULSE and GIS: an application mode for Calabria (southern Italy). Geomorphology 112: 228–245.

Ugur Ozcan A., Erpul G., Basaran M. & Emrah Erdogan H., 2008. Use of USLE/GIS technology integrated with geostatistics to assess soil erosion risk in different land uses of Indagi Mountain Pass-Çankırı, Turkey. Environ Geol (2008) 53:1731–1741. doi: 10.1007/s00254-007-0779-6.

Van der Knijff J.M., Jones R.J.A. & Montanarella L., 2000. Soil Erosion Risk Assessment in Europe. EUR 19044 EN. Office for Official Publications of the European Communities, Luxembourg, p. 34.

Wang G., Gertner G., Fang S. & Anderson A.B., 2003. Mapping multiple variables for predicting soil loss by geostatistical methods with TM images and a slope map. Photogramm Eng Remote Sens 69:889–898.

Wang G., Yu J., Shrestha S., Ishidaira H. & Takeuchi K., 2010. Application of a distributed erosion mode for the assessment of spatial erosion patterns in the Lushi catchment, China. Environ Earth Sci 61:787–797. doi: 10.1007/s12665-009-0391-z.

Wischmeier W.H., Smith D.D. (1958) – *Rainfall energy and its relationship to soil loss.* Amer. Geophysical Union Transactions of the ASAE, 12.

Wischmeier W.H., Smith D.D. (1960) – *A universal soil loss estimation equation to guide conservation farm planning.* Trans. 7th Congr. Int. Soil Sci. Soc. 1.

Wischmeier W.H. & Smith D.D., 1978. Predicting rainfall erosion loss: a guide to conservation planning. Agricultural Handbook No. 537, US Department of Agriculture, Agricultural Research Service, Washington, DC. 407 p.

Yue-Qing X., Xiao-Mei S., Xinag-Bin K., Jian P. & Yun-long C., 2008. Adapting the RULSE and GIS to model soil erosion risk in a mountains karast watershed, Guizhou Province, China. Environ Monit Assess (2008) 141:275–286. doi: 10.1007/s10661-007-9894-9.

Zhou P., Luukkanen O., Tokola T. & Nieminen J., 2008. Effect of vegetation cover on soil erosion in a mountainous watershed. Catena 75:319–325.

Received at: 12. 02. 2015
Revised at: 09. 09. 2015

Accepted for publication at: 06. 11. 2015
Published online at: 09. 11. 2015